Paste 2019 – AJC Paterson, AB Fourie and D Reid (eds)

Earth observation data and satellite InSAR for the remote monitoring of tailings storage facilities: a case study of Cadia Mine, Australia

A Thomas *CGG Services (UK) Ltd, UK*

SJ Edwards *University College London, UK*

J Engels *Tailpro Consulting, Chile*

H McCormack *CGG Services (UK) Ltd, UK*

V Hopkins *CGG Services (UK) Ltd, UK*

R Holley *CGG Services (UK) Ltd, UK*

Abstract

Tailings storage facilities (TSFs) are an essential infrastructure of mineral processing, but they represent a significant physical, chemical and biological hazard and must, therefore, be strictly and responsibly sited, managed and closed. Tailings can, for example, be dispersed by many processes (such as sinkholes, earthquakes, intense rainfall and flood events, and wind), substandard design and construction, and seepage. The stability and behaviour of TSFs needs to be continuously monitored and one highly effective way of doing this is through satellite Earth observation (EO).

The EO industry is witnessing a technological revolution. Large and long-lifespan satellite sensors that have been the staple of national space agencies and commercial satellite manufacturers are now being complemented by constellations of low-cost, short-lifespan 'cube sats' by companies with the ambition to image the whole earth daily. Satellites with synthetic aperture radar (SAR) sensors are also collecting high volumes of data, with the added benefit of being able to do so day or night and in different weather conditions. The range of data options and capabilities these provide open opportunities for novel data analysis techniques for TSFs. One of these is satellite InSAR (interferometric SAR; a technique used to map millimetric-precision changes in ground height over time), which is already used by mining companies to reduce risk in and of their operations. From monitoring the stability of TSFs, through to assessments of impacts of natural hazards, InSAR allows rapid and accurate targeting of high-risk areas and structures to identify those that require subsequent investigation through ground-based methods.

To demonstrate the application of EO data and InSAR in identifying pre- and post-failure mine activities and TSF deformation, the authors will present a case study across Cadia mine, New South Wales, Australia, which had a localised TSF failure on 9 March 2018. The InSAR results presented show that low-magnitude subsidence signals were observed across the TSF dam during the year preceding the collapse. In January 2018 a notable change in behaviour was observed, with a concentrated area of subsidence focused on the region which initially failed on 9 March 2018. Furthermore, post-collapse InSAR measurements show an increased rate of subsidence for regions either side of the failure zone. Review of medium- and high-resolution satellite images show that the failure was phased, with an initial failure and then a subsequent failure at least two days after 9 March 2018. It also highlights what might be construction activity associated with a dam raise prior to failure.

Keywords: *tailings, TSF, InSAR, satellite, slope stability, displacement, earth observation*

1 Tailings and their storage, failure and monitoring

The global demand for mineral commodities of the extractive industry is ever increasing. Along with the extraction of the valuable material comes a significant volume of residue that may exceed that of the targeted resource by at least one to two orders of magnitude. The main residue constitutes tailings, which are mixtures of finely ground rock and fluid from mineral processing. The volume and potential toxicity of tailings present a huge challenge for their effective management, which should ensure that they are safely isolated from the environment. However, this has been or is achieved to different levels of success in a number of ways that include riverine and submarine disposal, retention in wetlands, backfilling, dry stacking and storage in dammed impoundments (Lottermoser 2007). There is a legacy of abandoned or poorly managed tailings, but increasingly stringent requirements mean that dammed impoundments are widely used, particularly by large companies in the developed world (Kossoff et al. 2014). These structures are often referred to as tailings storage facilities (TSFs) and the majority contain slurries, but paste, thickened and filtered tailings are also stored. The retention wall or embankment is often constructed from the coarse sand fraction of the tailings, with the finer fraction deposited in the reservoir behind and covered by water to suppress dust and acid-generating oxidation reactions. After construction of the initial starter embankment, the embankment is progressively raised in a series of lifts where the crest moves upstream, vertically (centreline) or downstream (Vick 1983).

Perhaps the greatest risk to a mining operation is a tailings failure (Figure 1), because of the subsequent environmental, human, economic and political impacts (Kossoff et al. 2014). It is estimated that each year there are on average two reported and two unreported tailings incidents (Commonwealth of Australia 2016) and the global distribution of these and the main causes of failure are summarised in Figure 2. Rico et al. (2008) suggests that active, rather than inactive, TSFs are most likely to fail, with the upstream structure most vulnerable. The scale and damage of such incidents were recently exemplified by the 2014 Mount Polley (British Columbia, Canada), 2015 Samarco Fundão and 2019 Córrego do Feijão barragem 1 (Minas Gerais, Brazil) disasters. These three events acted as a catalyst for renewed efforts to better manage TSFs through design, maintenance and monitoring, to ensure they are performing adequately and not presenting a hazard.

Figure 1 Examples of tailings storage facility failures: (a) shows the July 2017 failure of the Mishor Rotem mine, Israel (Copyright REUTERS/Baz Ratner 2017); (b) shows the November 2015 failure of Samarco/Bento Rodrigues, Brazil (Copyright Corpo de Bombeiros/MG 2015); (c) shows the October 2010 failure of Kolontar, Hungary. Photos sourced from AGU The Landslide Blog (2018)

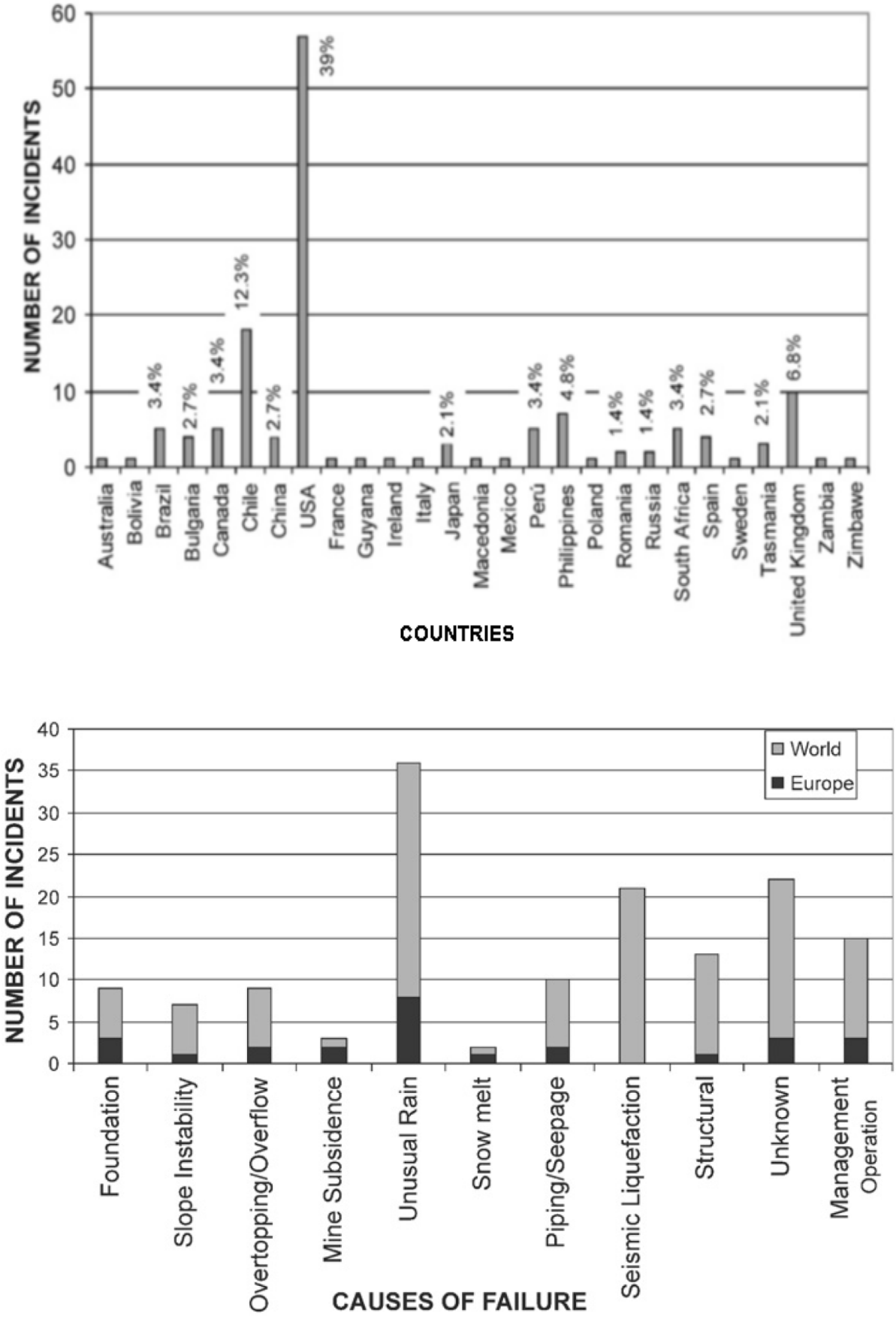

Figure 2 Global distribution and causes of tailings incidents reproduced from Rico et al. (2008)

Most TSF failures, other than those initiated by earthquakes or extreme weather events, are usually preceded by warning signs that must be detected as early as possible (Martin and Davies 2000). Increasingly, remote monitoring is being used; and in this paper we briefly outline the benefits of Earth observation (EO) data and satellite InSAR (interferometric synthetic aperture radar). We then apply these tools to analyse the March 2018 partial failure of the northern TSF at the Cadia gold operation of Newcrest Mining in Orange, New South Wales, Australia.

1.1 TSF monitoring

There are a range of monitoring techniques currently applied to TSF management that focus on detecting operational anomalies, provide a means of early detection/warning, and optimise the day-to-day operational planning. Some of the main methods currently used are:

- Manual onsite inspections:
  - Daily operational visual inspection sheets (TSF operators).
  - Specialist inspections (geotechnical and civil engineers).
  - Third-party review and audits.
- Remote sensing:
  - Medium-to-high resolution optical satellite imagery.
  - Satellite InSAR ground stability surveying.
  - Ground-based InSAR systems.
  - Unmanned aerial vehicles (UAV).
- Closed circuit television (CCTV) and time-lapse photography.
- Instrumentation and telemetry.

A good TSF monitoring plan utilises a combination of these methods to provide a more robust monitoring program, rather than relying on a single technology or manual inspection. Instrumentation, together with real-time telemetry and satellite-based services, have increased in their use for TSF monitoring, particularly over the last decade. The reliability of instrumentation and the life-span of sensors installed in TSFs have also improved dramatically over recent years, as well as a reduction in the costs of acquiring and installing such equipment.

Instrumentation can provide a control room operator with an early warning mechanism to reduce or prevent the possibilities of a more catastrophic event occurring. For example, detection of a tailings pipe rupture would result in the instantaneous shutdown of the delivery line. Likewise, measurement of piezometric levels of a main embankment could allow mitigation techniques to be applied prior to saturation of the embankment toe, which would otherwise only be detected via a manual visual inspection. However, data from instrumentation within a TSF must be reviewed and interpreted to ensure that the equipment is monitoring correctly, and that the results of the various instruments and sensors are within acceptable short- to long-term limits (both regulatory and operationally).

Satellite services, particularly InSAR, provide a good third-party review of how a TSF is performing and if any potential anomalies are occurring that may not be obvious to the operators or mine management. InSAR provides an external review of any potential deformation of a TSF, such as embankment movement or sinkhole development (as a proxy from their wider deformation field), and can provide a reliable early warning system with millimetric precision. The following sections of this paper provide a more in-depth review of TSF monitoring using InSAR and the additional value that can be derived from optical satellite imagery.

1.2 Satellite interferometric synthetic aperture radar

SAR is a type of active remote sensing instrument that uses the microwave region of the electromagnetic spectrum. Although SAR instruments may be used in airborne or terrestrial contexts, for the applications considered here, satellite-based SAR instruments predominate. SAR instruments transmit a series of radar pulses and record the reflections from the Earth's surface. This returned signal is then processed to form an image with each pixel containing the radar response of a particular location.

Amplitude is the strength of the radar response. This is typically affected by the backscatter characteristics of the surface. Phase is the fraction of a complete sine wave cycle. Since the outgoing wave is produced by the SAR instrument, the phase is known, and can be compared to the phase of the return signal. The phase of a SAR signal depends on a complex interaction of surface properties, which vary from pixel to pixel, so a single SAR phase image appears to contain random noise.

Satellite InSAR compares the phase values in different SAR images for the same point on ground, generating the interference between returned phase values to produce an interferogram. If surface properties have stayed the same between the two SAR images the phase signals cancel out, leaving only the phase differences due to properties that have changed. Phase differences between SAR images appear in an interferogram as a series of 'fringes'. These fringes are directly related to the radar wavelength. Differences in interferometric phase (phase shifts) can be caused by several factors, but the most important stems from changes in the path length (the distance to the ground and back), which is directly linked to topography and topographic change (i.e. deformation). The path length consists of several whole wavelengths plus a fraction of a wavelength. The total path length (i.e. the number of whole wavelengths) is not known, but the phase provides an extremely accurate measure of this extra fraction of a wavelength.

Satellite InSAR exploits the temporal separation between SAR data acquisitions, time periods in which deformation (movement towards or away from the SAR sensor) may have occurred (resulting in a phase shift). Displacements are measured along an inclined line of sight (LOS), meaning they are sensitive to a combination of vertical and east–west displacement. InSAR measurements also rely on the surface properties remaining the same across a period of time. Any substantial disturbance of the surface, for example movement of earth, construction or thick vegetation growth, can result in higher uncertainties or loss of coverage in the affected areas. This is measured using coherence, a spatial measure of the level of noise, with low coherence representing increased noise and loss of coverage.

1.3 Cadia tailings storage facility failure

Cadia Valley Operations (CVO) is one of Australia's largest gold operations. The mine is located in central western New South Wales, approximately 25 km from the city of Orange, and 250 km west of Sydney.

CVO has been in operation since the 1990s and comprises three mines: Cadia East underground panel cave mine which commenced commercial production on 1 January 2013, the Ridgeway underground mine and the Cadia Hill open pit mine. The latter two mines are currently on care and maintenance.

Figure 3 shows the key regions of the mine. The main focus of this paper is on the two TSFs labelled 4 and 5.

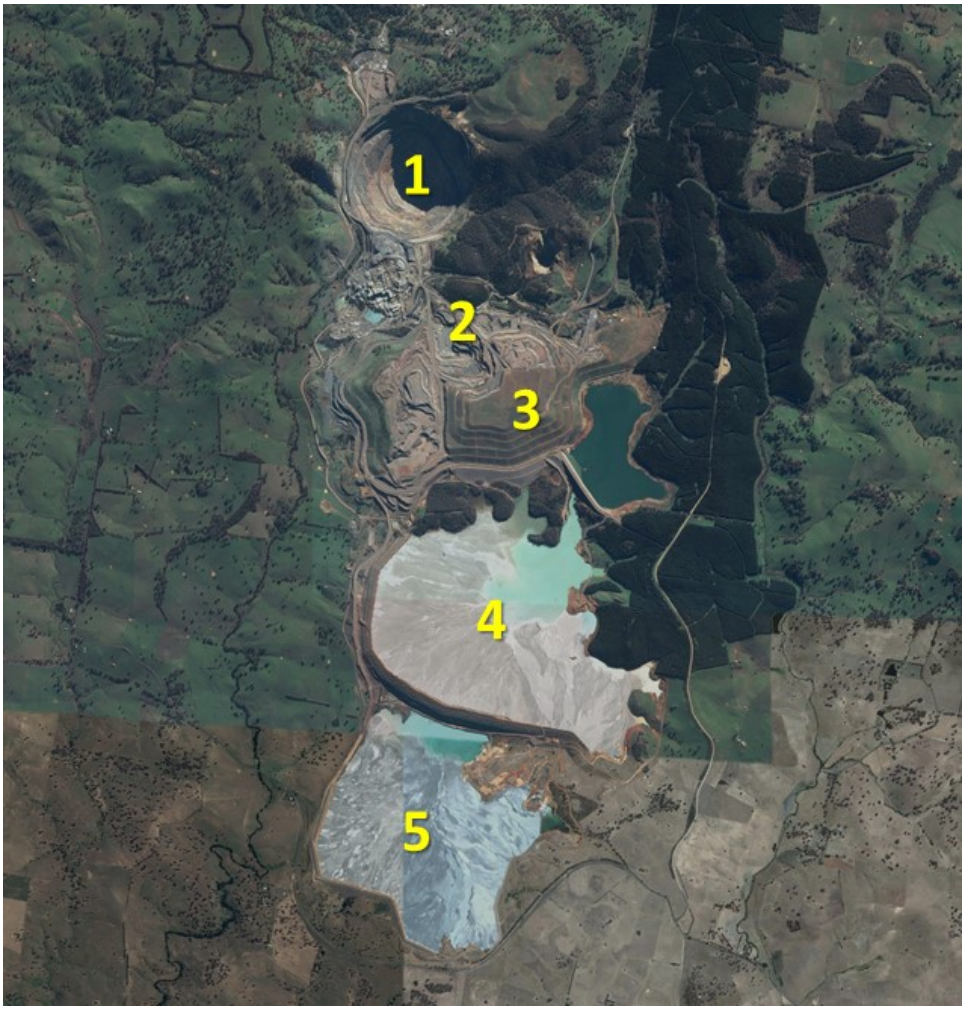

Figure 3 **Overview map of Cadia Valley Operations site: (1) Cadia Hill open pit; (2) Cadia East underground mine; (3) South Waste Rock Dump; (4) Northern tailings storage facility; (5) Southern tailings storage facility. Image copyright DigitalGlobe, CNES/Airbus (Alphabet Inc. 2018)**

On 9 March 2018 a news release issued by Newcrest Mining announced that a limited breach of the northern TSF had taken place. The failure was contained within the southern TSF. It measured ~270 m across, with a back-scar from the crest of the dam measuring ~100 m and the main slump event measuring ~370 m (Figure 4).

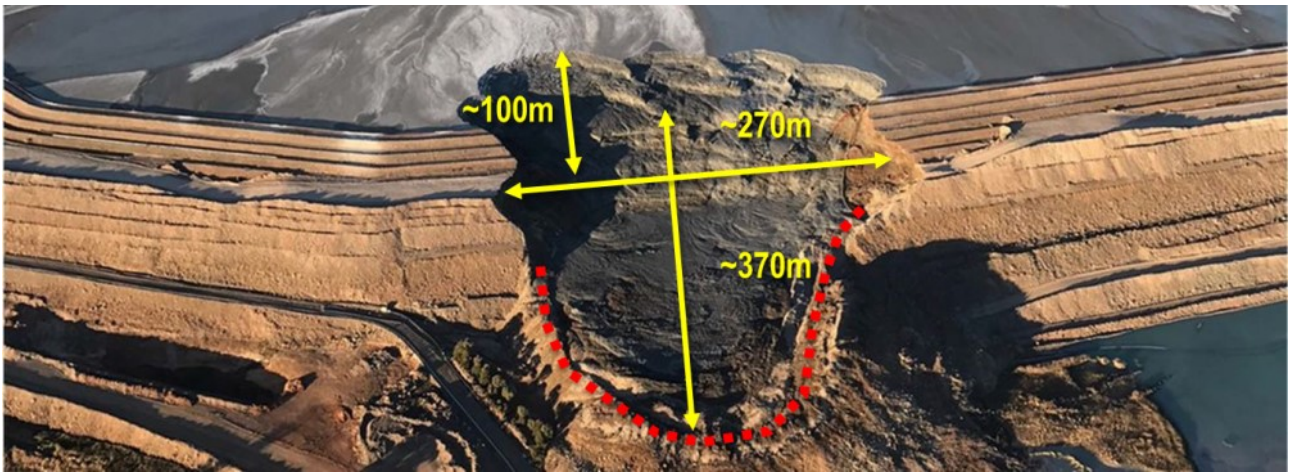

Figure 4 **Aerial photo of failure and estimated dimensions. Image sourced and modified from Newcrest Mining Ltd. (2018)**

The day before the failure, two 2.5 magnitude earthquakes took place. There is no evidence to suggest that these seismic events were responsible for the failure, however it is worth noting that in 2017 a 4.3 magnitude earthquake struck in the vicinity of the mine leading to six months of disruption to mine operations, but there is no evidence to suggest that the TSFs were impacted at that time.

On the morning of 9 March cracks were observed on the dam wall, and at approximately 7.00 pm local time the failure is believed to have occurred. Site operations were suspended on 10 March and on the 15 March full-time monitoring of the TSF was implemented using a GroundProbe™ slope stability radar system. Mining and processing recommenced on 27 March 2018. On 23 April Newcrest received permission to use the open pit (Figure 3) to dispose of tailings, and on 7 May disposal commenced.

2 Methodology

Freely available Sentinel-1 SAR data from the European Space Agency (ESA), enabled an historical study to be performed whilst offering the possibility for ongoing monitoring of the TSF. The Sentinel-1 data archive spans 2015 through to the present day, with images acquired at 12-day intervals at ~25 m spatial resolution.

Compared to similar satellites, Sentinel-1 data provides good coherence due to a frequent acquisition cycle and precise orbit control. This typically allows successful unwrapping of the data, to provide maps of displacement for each period, maps of mean displacement rate over longer periods of time, and the ability for time series analysis showing the variation in the deformation rate through time for each location.

Two separate epochs were chosen (pre-collapse from 1 March 2015 to 9 March 2018, and post-collapse from 21 March 2018 to 18 July 2018) to evaluate the post-failure stability of the TSF. Deformation occurring during the collapse events could not be measured using InSAR, since the large surface change results in poor coherence and complete loss of coverage. However, this area of low coherence does delineate the extents of the failure.

A network of interferograms were formed between each available SAR image within the two-time epochs. Adaptive spatial averaging was applied to reduce noise while preserving boundaries between different surface features. Atmospheric artefacts were removed by applying a long wavelength spatial filter to the data, removing the wide-scale atmospheric signals but allowing the deformation signals through. One SAR image from 14 April 2018 showed significant atmospheric anomalies and was removed from processing.

Unwrapping of the interferograms was successful across most areas of the TSF, except for the wet tailings pond areas where coherence was too low. Vegetated areas away from the TSF also had limited coherence. The network of interferograms was checked visually and statistically to identify and remove any areas where unwrapping was inconsistent and potentially incorrect.

The stack of unwrapped interferograms were then combined to provide a time series of sequential measurements of displacement, through each of the two epochs. This can be visualised spatially as a map of displacement between any two time periods, or through time showing the evolution of displacement for a particular pixel.

The data were acquired from a descending orbit with an incidence angle of ~33°, meaning displacements towards the satellite may represent a combination of upward and/or eastward components of motion, and displacements away from the satellite represent downward and/or westward motion. The measurements are more sensitive to vertical than horizontal displacement, therefore for simplicity the terms uplift and subsidence have been used to describe displacement towards and away from the satellite, respectively.

3 Results and discussion

3.1 Precursor deformation

SAR data acquired prior to the failure on 9 March 2018 was analysed to determine whether any precursor deformation was observable. A total of 81 descending Sentinel-1 SAR images were used to generate interferograms. During processing it was noted that winter-spanning interferograms (i.e. May to September) generally had a better coherence than the summer interferograms (November to February). This is due to seasonal variation in the vegetation local to the mine.

The interferograms were then combined to form a time series of displacement to evaluate long-term, precursor deformation trends across the TSF. The time series show a series of transient low-magnitude subsidence signals at various locations along the tailing dam over the preceding months progressing from the western part of the dam down towards the failure location. There is also a steady low-magnitude subsidence signal observed around the inner edge of the tailings dam throughout the period. These may potentially represent consolidation of the dam material, or changes in stress due to tailings deposition.

In mid- to late-January 2018, a change in behaviour was apparent, with a stronger concentrated area of subsidence focused on the area of eventual failure (Figure 5). The time series graph (Figure 6) indicates that deformation was occurring at this location as far back as March 2017, with a displacement of around 10–20 mm up to December 2017. In late January 2018, an accelerating period of progressive deformation began, with 29 mm of displacement occurring between 20 January and 25 February 2018, prior to cracks being observed on the morning of 9 March 2018 and failure that same evening.

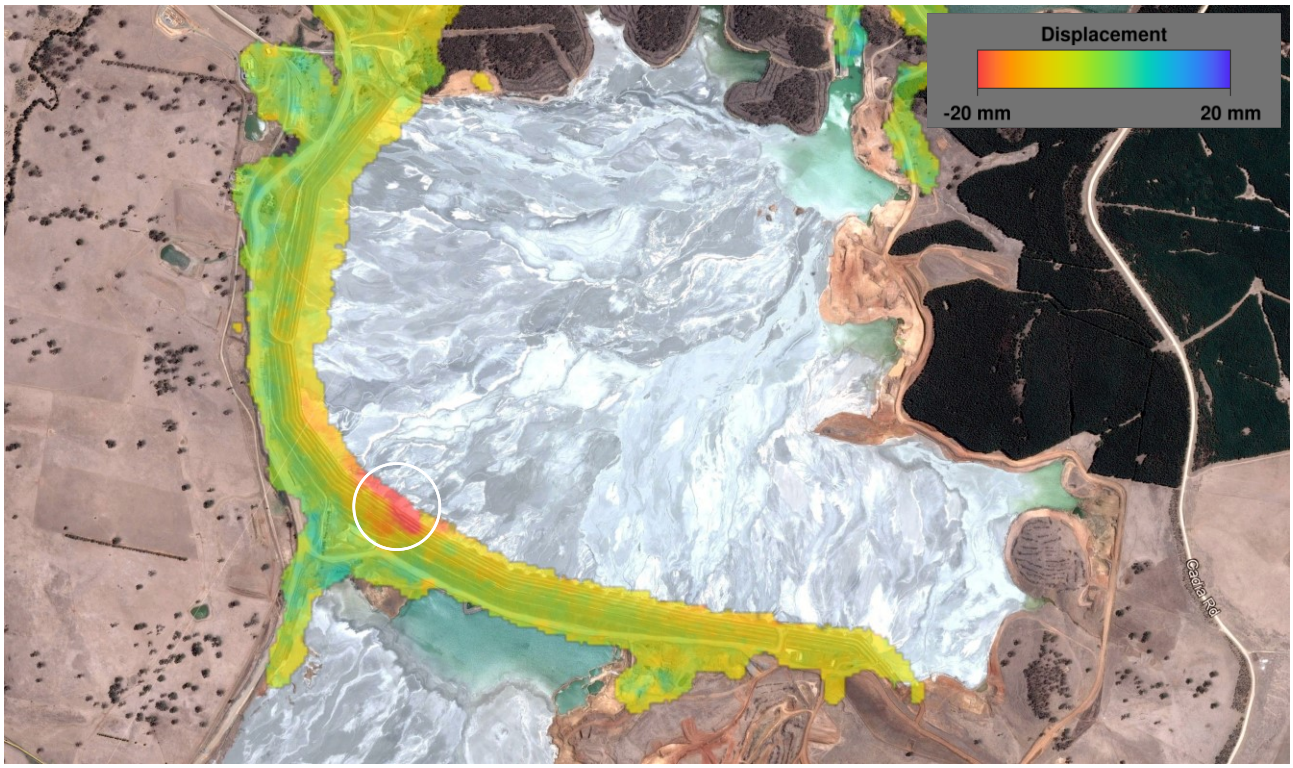

Figure 5 Displacement map spanning 20 January 2018 to 25 February 2018. Failure zone denoted by the white circle, Background imagery © CNES/Airbus (Alphabet Inc. 2018). InSAR data contains modified Copernicus Sentinel data (2018), © CGG 2018

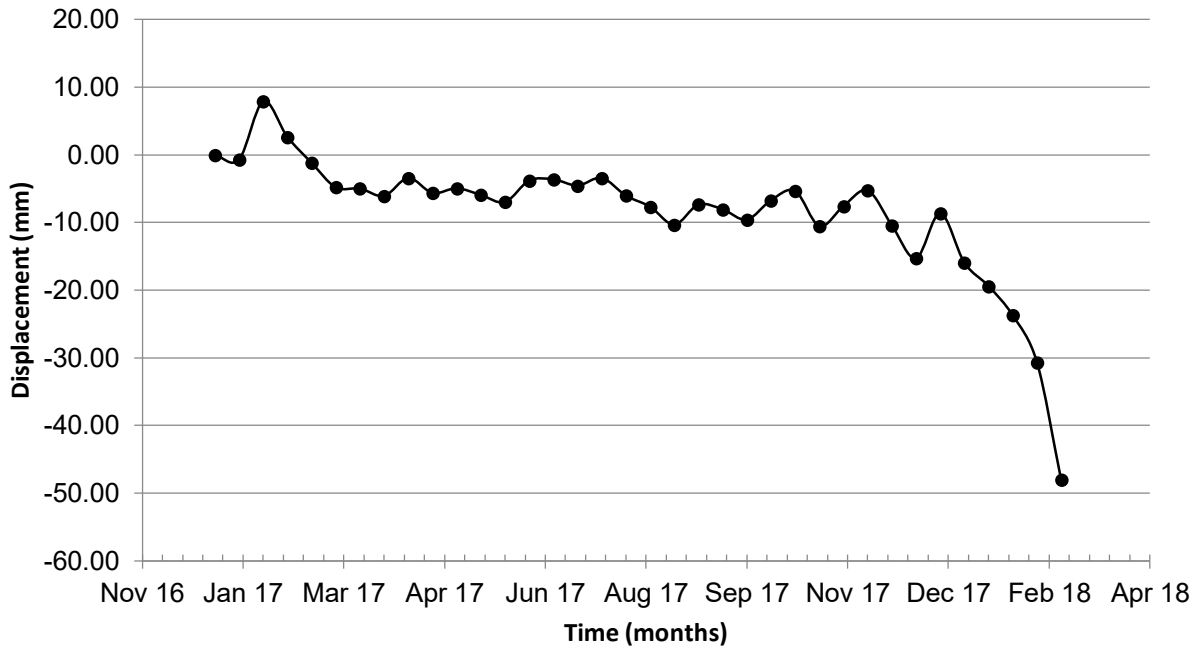

Figure 6 Time series of displacement for a pixel located within the subsiding region shown in Figure 5, © CGG 2018

Where accelerating displacements are detected, a widely-used method to estimate the timing of eventual failure is based on calculation of the inverse velocity (e.g. Carlà et al. 2017). In this model, a plot of the inverse of the velocity will show progressively smaller values as displacement accelerates, and a linear extrapolation of this relationship can be used to estimate when the inverse velocity approaches zero, i.e. when velocity becomes very large and failure is inevitable.

Figure 7 shows the time series of the inverse velocity for the period between 20 January and 25 February 2018. There is a clear trend of increasing acceleration, and extrapolating these results show that failure (an inverse velocity approaching zero) is predicted approximately two days before the failure occurred.

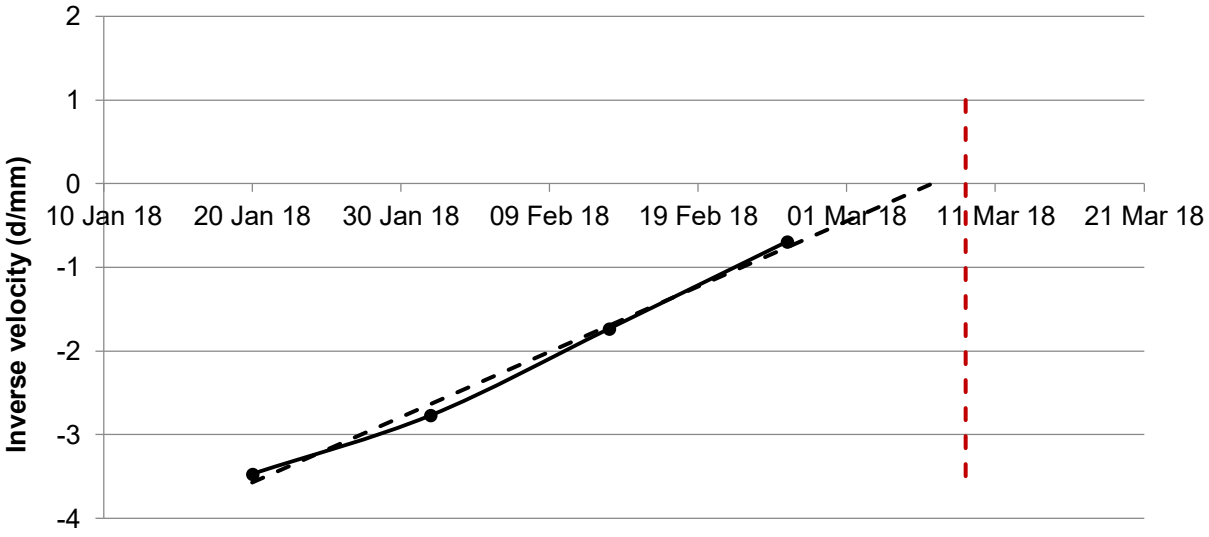

Figure 7 Time series of inverse velocity, calculated for the same location as Figure 6, © CGG 2018

3.2 Pre-failure dam construction

High resolution satellite imagery (53 cm, WorldView-2) acquired at 10.28 am local time on 9 March 2018 indicates that construction activity was taking place on the northern TSF dam wall on and/or before the day of failure (Figure 8). The imagery appears to show evidence of a dam raise – a process of increasing the height of the dam wall to increase the overall capacity of the TSF. The visual evidence of a newly graded surface and the presence of a bulldozer to the east of the dam wall suggests this may be the case.

Figure 8 WorldView-2 imagery acquired at 10.28 am local time on 9 March 2018. White circles indicate construction activity, © DigitalGlobe 2018

3.3 Failure

Optical satellite imagery (Sentinel-2, 10 m resolution) shows that the failure occurred in two stages. Imagery acquired on 11 March 2018 shows the boundary of the initial failure (Figure 9), however a second Sentinel-2 image acquired on 14 March 2018 shows a secondary failure that occurred at the same location (Figure 9).

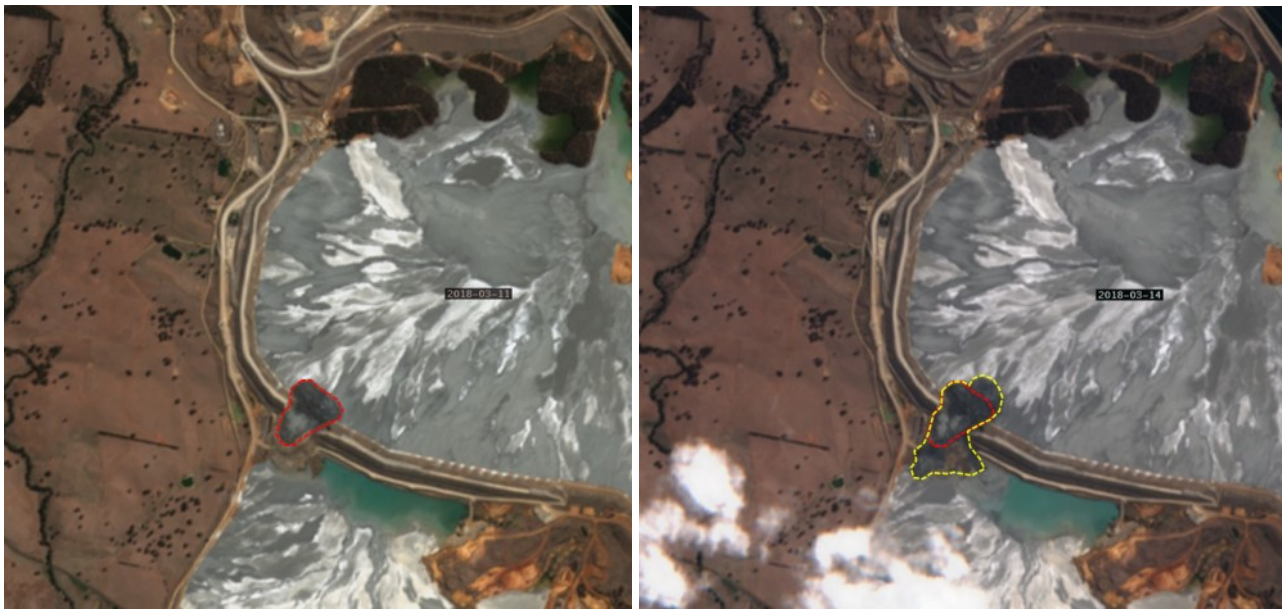

(a) (b)

Figure 9 Sentinel-1 imagery acquired on (a) 11 March 2018, with the boundary of the initial failure indicated by the red polygon; (b) 14 March 2018 with the secondary failure indicated by the yellow polygon. © Contains modified Copernicus Sentinel data (2018), CGG 2018

3.4 Post-failure deformation

In the post-collapse analysis ten new descending SAR images were acquired by the Sentinel-1 satellites at 12-day intervals from 21 March until 19 July 2018 and processed. The aim of this was to establish whether the TSFs had stabilised post-collapse or whether they were still moving.

Figure 10 shows the mean displacement rate for the TSFs post-collapse. The red and orange regions on the map show where the TSF dam was still subsiding following the collapse, with the highest amount change occurring in the regions surrounding the failure. The greatest subsidence occurred in the region to the east of the failure (red area) with displacements of up to 40 mm over the time period. This region of the tailings is notably subsiding more compared to the pre-collapse event measurements, implying that it could be under additional stress following the collapse.

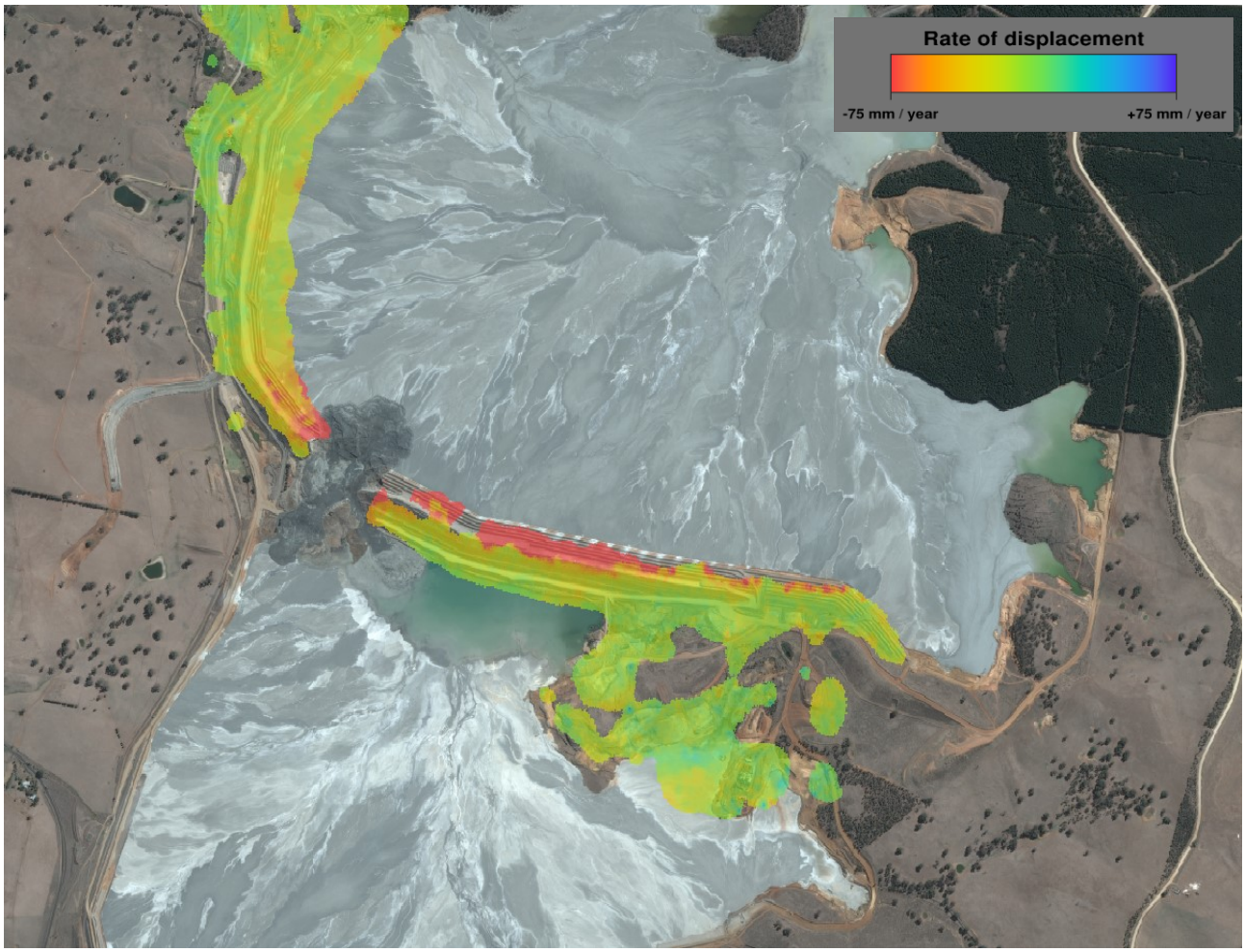

Figure 10 Rate map showing the mean displacement rate of tailings storage facilities from 21 March to 19 July 2018. The red and orange regions show where the tailings storage facility dam was still subsiding following the collapse. Background imagery © CNES 2018, Distribution Airbus DS. InSAR data contains modified Copernicus Sentinel data (2018), © CGG 2018

Figure 11 shows a time series of cumulative displacements from the region just to the west of the collapse. This area was still significantly subsiding post-collapse, with a maximum measured deformation of 23 mm at this location. The rate of change of displacement reduces from June 2018 onwards implying the region is beginning to decelerate and possibly start stabilising.

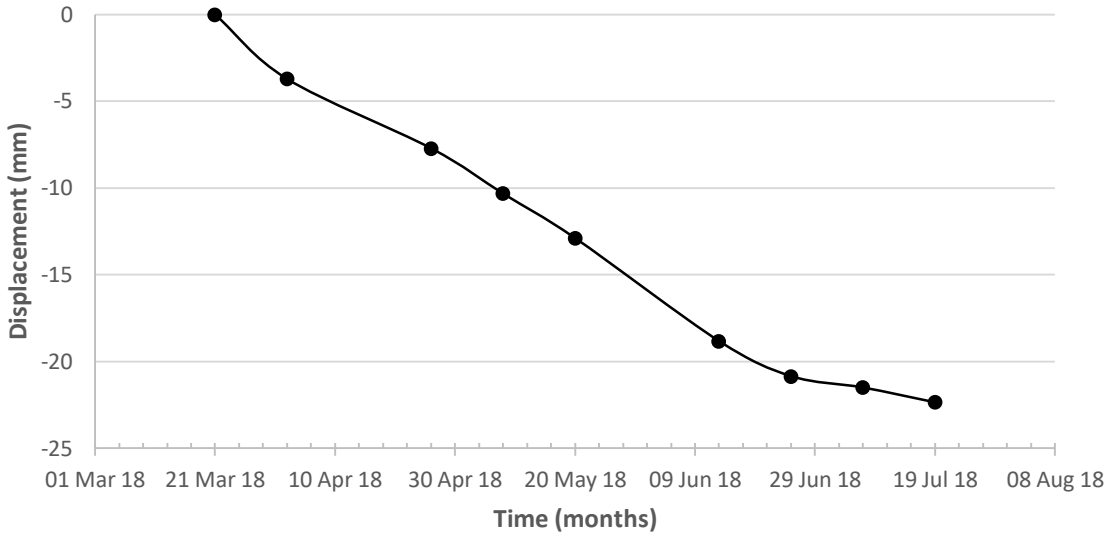

Figure 11 Displacement time series showing the cumulative displacement against time from 21 March to 19 July 2018 for the area of the tailings dam just to the west of the failure. © CGG 2018

The uncertainty in the data for the post collapse analysis is 3.3 mm at a 95% confidence level. This is based on the stable areas of the region assuming a normal distribution of the data.

Overall, the post-collapse results show, at the time of writing, that the dam was still subsiding after failure occurred. The rate of acceleration appeared be decreasing, however more data from ongoing monitoring would be required to confirm whether the region is stabilising.

4 Conclusion

In this paper we demonstrate how EO data – optical imagery and satellite InSAR measurements – can be a valuable tool in providing greater insight into site activities and long-term deformation behaviour across TSFs.

The InSAR results presented show that some low-magnitude subsidence signals were observed at various locations across the TSF dam during the year preceding the collapse, exhibiting a mixture of transient and progressive displacement. In mid- to late-January 2018, a notable change in behaviour was observed, with a stronger concentrated area of subsidence focused on the area of eventual failure.

This area exhibited progressive acceleration through February 2018, which ultimately culminated with the initial failure on 9 March 2018. Analysis of the observed acceleration using an inverse velocity method showed a good fit between modelled and actual date of the failure. Furthermore, post-collapse InSAR measurements show an increased rate of subsidence for areas either side of the failure zone, relative to the pre-event background rates. There is some initial indication that this rate may have been decreasing at the time of writing this paper.

Review of medium- and high-resolution satellite images, acquired by Sentinel-2 and WorldView-2 respectively, reveals some important observations about the site that weren't communicated by Newcrest. Firstly, two Sentinel-2 images acquired shortly after the failure show that the event was phased, with an initial failure and then a subsequent failure at least two days after 9 March 2018. Although this is interesting in its own right and may help determine the cause of the failure, it also serves to highlight how unpredictable these types of hazards can be. As such, using satellite data presents a clear advantage for remotely mapping and monitoring such locations, without putting personnel and expensive ground-based sensors at risk. Secondly, high resolution WorldView-2 imagery indicates what might be construction activity associated with a dam raise prior to failure.

EO data is increasingly being used by mining companies and this paper justifies why this should form an integral part of a mines' monitoring program. The example across Cadia demonstrates the benefit that satellite InSAR can provide to operational mines, in terms of its ability to remotely monitor TSFs (and other assets) on a frequent basis, with the aim of informing and complementing ground-based sensor networks and geotechnical assessments, and de-risking mine operations to ensure continuity in production.

Acknowledgement

InSAR results contain modified Copernicus data, 2017–2018.

Author SJ Edwards acknowledges financial assistance from the UK Foreign & Commonwealth Office Global Britain Fund to support his engagement with CGG Services (UK) Ltd. and Tailpro Consulting (Chile).

References

AGU The Landslide Blog 2018, https://blogs.agu.org/landslideblog

Alphabet Inc. 2018, *Google Earth Pro*, version 7.3.2.549, computer program, viewed 7 February 2019, https://www.google.com/earth

Carlà, T, Intrieri, E, Di Traglia, F, Nolesini, T, Gigli, G & Casagli, N 2017, 'Guidelines on the use of inverse velocity method as a tool for setting alarm thresholds and forecasting landslides and structure collapses', *Landslides*, vol. 14, no. 2, pp. 517–534.

Commonwealth of Australia 2016, *Tailings Management*, Leading Practice Sustainable Development Program for the Mining Industry Handbook Series, Australian Government.

Copernicus satellite data (open access), ESA Open Access Hub, https://scihub.copernicus.eu

Kossoff, D, Dubbin, WE, Alfredsson, M, Edwards, SJ, Macklin, MG & Hudson-Edwards, KA 2014, 'Mine tailings dams: characteristics, failure, environmental impacts, and remediation', *Applied Geochemistry*, vol. 51, pp. 229–245, http://dx.doi.org/10.1016/j.apgeochem.2014.09.010

Lottermoser, B 2007, *Mine Wastes: Characterization, Treatment and Environmental Impacts*, Springer-Verlag, Heidelberg.

Martin, TE & Davies, MP 2000, 'Trends in the stewardship of tailings dams', *Proceedings of the Seventh International Conference on Tailings and Mine Waste*, A.A. Balkema, Rotterdam, pp. 393–407.

Newcrest Mining Ltd. 2018, http://www.newcrest.com.au/news-and-information

Rico, M, Benito, G, Salgueiro, AR, Díez-Herrero, A & Pereira, HG 2008, 'Reported tailings dam failures: a review of the European incidents in the worldwide context', *Journal of Hazardous Materials*, vol. 152, pp. 846–852.

Vick, SG 1983, *Planning, Design, and Analysis of Tailings Dams*, John Wiley & Sons, New York.